

Toxic Interaction Mechanism of food Colorant Sunset Yellow with trypsin by Spectroscopic and Computational Method

Hongcai Zhang, Baosheng Liu*, Xu Cheng

College of Chemistry & Environmental Science, Hebei University, Baoding 071002, Hebei Province, P. R. China

*corresponding author: E-mail: lbs@hbu.edu.cn.

Abstract— The interaction between food colorant sunset yellow (SY) and trypsin (TRP) was studied by multiple spectroscopic and molecular docking methods and molecular docking simulation under simulated physiological conditions to evaluate the toxic of SY at the protein level. The results showed that SY could effectively quench the endogenous fluorescence of TRP, formed a 1:1 complex. The binding distance (r) between SY and TRP was obtained based on the Förster nonradioactive resonance energy transfer and r was less than 7 nm, which indicated that there was a non-radiative energy transition in the system. The thermodynamic parameters were obtained from the van't Hoff equation, and the Gibbs free energy $\Delta G < 0$, indicating that the reaction was spontaneous; $\Delta H < 0$, $\Delta S > 0$, indicating hydrophobic interaction played a major role in forming the SY-TRP complex. Molecular docking results showed that SY was surrounded by the active amino acid residues Ser195, His57 and Asp102 of TRP, which altered the microenvironment of amino acid residues at the catalytic active center of TRP. Furthermore, as shown by the synchronous fluorescence, UV-Visible absorption and circular dichroism data, SY could lead to the conformational and microenvironmental changes of TRP, which may affect its physiological function.

Keywords— Spectroscopy; Sunset yellow; Trypsin; Molecular docking; Binding rate.

I. INTRODUCTION

Trypsin (referred to as TRP) is a serine protease with a molecular weight of 24,000 Da, which is widely found in the pancreas and is an important digestive protease in humans [1]. TRP owns about 223 amino acid residues and consists of two size close tubbiness structural domains which were connected by six disulfide bonds. Every domain have six antiparallel of β -foldings and between two of domains are His57, Asp102 and Ser195 which are catalytic activity center of TRP, the three of structures above form catalysis triplet [2]. TRP has diverse biological functions such as immune responses, digestion and hemostasis [3].

Sunset yellow (SY, structural formula was shown in Fig. 1) is a synthetic acid azo dye. Due to the presence of two

sulfonate groups at both ends of the molecule, it is significantly soluble in aqueous solution. It is widely used in the beverage, confectionery, pastry, brewing, pharmaceutical and cosmetic industries as a coloring agent [4]. The metabolism of SY in the human body will produce harmful β -naphthol and other products. The maximum daily intake accepted by the FDA (Food and Drug Administration) is 225 mg for a 60 kg person [5]. Long-term consumption of food exceeding the standard of SY will aggravate the burden on the liver of the human body and damage to liver function [6]. Some studies have shown that the long-term intake of SY will affect the intelligence level of children, leading to behavioral disorders such as ADHD, and in severe cases can even cause cancer [7].

In recent years, fluorescence spectroscopy has become an important method for studying the interaction of small molecules and proteins. So far, Mohseni-Shahri *et al.* used spectroscopy to study that SY quenched the fluorescence of pepsin by static quenching [8]. Liu Zhidong *et al.* determined that SY and bovine serum albumin form an approximate 1:1. complex [9]. While TRP is an important digestive protein in human body, when the SY with water and food gets into the body, the first place it enters is the digestive system and become bound to the digestion enzymes before they can go into the blood plasma. Therefore, the interaction between SY and TRP was studied by using multiple spectroscopy methods and molecular docking techniques. The results may be helpful to complement the limited toxicity literature for SY, and will also provide a new approach to probe the toxicity of SY at the molecular level.

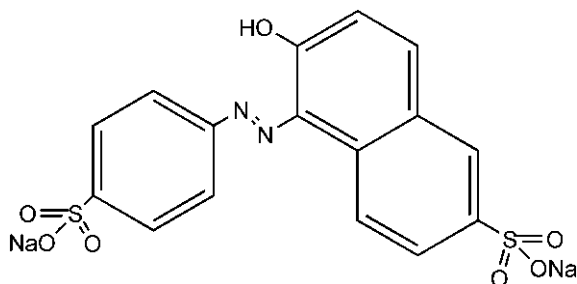


Fig.1 Chemical structure of SY

II. EXPERIMENTAL

2.1 Apparatus

These fluorescence spectra were acquired with a Shimadzu RF-5301PC spectrofluorophotometer. Circular dichroism spectra were recorded on a MOS-450/SFM300 circular dichroism spectrometer (Bio-Logic, France). Absorption was measured with an UV-vis recording spectrophotometer (UV-3600, Shimadzu, Japan). All pH measurements were made with a PHS-3C precision acidity meter (Leici, Shanghai, China). All temperatures were controlled by a SYC-15_B superheated water bath (Sangli, Nanjing, China).

2.2 Materials

TRP (Sigma Company), solution (2.0×10^{-5} M) was prepared. SY standard solution (1.0×10^{-3} M) was prepared. Tris-HCl buffer solution was used to keep the pH of the

solution at 7.40, containing NaCl (0.15 M) to maintain the ionic strength of the solution. All other reagents were analytical grade and all aqueous solutions were prepared with newly double-distilled water and stored at 277 K.

The fluorescence intensity measured in the experiment was corrected by the "internal filter effect" Eq.(1) [10]:

$$I_{cor} = I_{obs} \times e^{(A_{ex} + A_{em})/2} \quad (1)$$

Where I_{cor} and I_{obs} are the fluorescence intensities corrected and observed, respectively, and A_{ex} and A_{em} are the absorption of the system at the excitation and the emission wavelength, respectively. The intensity of fluorescence used in this paper is the corrected fluorescence intensity.

2.3 Experiment procedure

2.3.1 Fluorescence measurements

The fluorescence measurements were performed as follows: 1.0 mL Tris-HCl buffer solution, 2.0 mL TRP (2.0×10^{-5} M), and different volume of SY were added into 10.0 mL colorimetric tube successively. The samples were diluted to scaled volume with double-distilled water, mixed thoroughly by shaking, and kept static for 30 min at different temperatures (298 K, 310 K, and 318 K). Excitation wavelength with excitation and emission slit at 5 nm for TRP was 280 nm and 295 nm, respectively. The fluorescence spectra were measured (emission wavelengths of 280-450 nm). At the same time fixed $\Delta\lambda=15$ nm or $\Delta\lambda=60$ nm, the synchronous fluorescence spectra of TRP and SY were recorded.

2.3.2 Circular dichroism measurements

A total of 1.0 mL Tris-HCl buffer solution, 2.0 mL TRP solution (2.0×10^{-5} M), and different volumes of SY were added into a 10.0 mL colorimetric tube successively. The concentration of trypsin was kept at 4×10^{-6} M while varying the SY concentration by keeping the molar ratios of SY to TRP as 1:0, 1:5 and 1:10. The samples were diluted to scaled volume with water, mixed thoroughly by shaking, and kept static for 30 min at 298 K. Each spectrum was recorded at wavelengths between 190 and 300 nm and a scan speed of 1 nm/s.

2.3.3 UV-vis measurements

1.0 mL Tris-HCl buffer solution (pH=7.40), 2.0 mL

Open Access

TRP solution (2.0×10^{-5} M) and different volume of SY were successively added to a 10.0 mL colorimetric tube, and the reference solutions were the corresponding concentration of SY solutions. The samples were diluted to scaled volume with water, mixed thoroughly by shaking, and kept static for 30 min at 298 K. The UV-vis absorption spectrum of SY in the presence and absence of TRP were scanned with 1cm quartz cells over the range from 190 nm to 400 nm.

2.3.4 Molecular docking

The two-dimensional structure of SY was drawn in ChemDraw 15.0, and its three-dimensional structure was optimized by model of molecular mechanics in ChemDraw 3D. The crystal structure of TRP used for molecular docking was obtained from protein data bank (PDB ID: 2ZQ1). Waters and all other HETATM molecules were removed from the TRP PDB file. Polar hydrogen atoms and Gasteiger charges were added to prepare the TRP molecule for docking. Protein-ligand docking was performed with the rigid docking tool in the Autodock 4.2.6, and the genetic algorithm is mainly used to calculate the possible conformation of SY combined with TRP[11].

III. RESULTS AND DISCUSSION

3.1 The Fluorescence spectra of SY-TRP system

At 280nm wavelength, the Trp and Tyr residues in TRP are excited, whereas a wavelength of 295nm excites only Trp residues [12]. Fig. 2 showed that the fluorescence emission spectrum of TRP when SY was added at different concentrations (the fluorescence emission spectrum of $\lambda_{ex}=295$ nm SY-TRP was similar, but the fluorescence intensity was lower). As shown in Fig. 2, the maximum fluorescence emission peak appeared at the wavelength of 337 nm, as the SY concentration increasing, the fluorescence quenching degree of TRP increased, and the maximum emission peak had a red shift, indicating that SY-TRP system interacted and generated a stable compound.

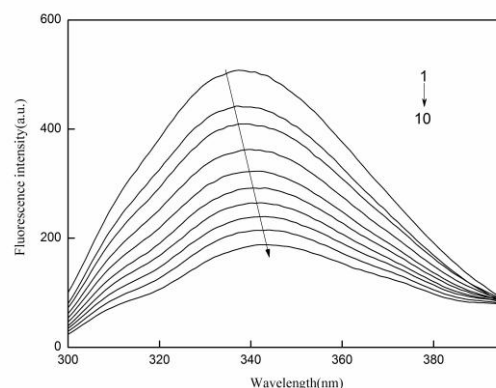


Fig.2 Fluorescence emission spectra of SY-TRP system

$$(T=298 \text{ K}, \lambda_{ex}=280 \text{ nm})$$

$$C_{\text{TRP}}=4.0 \times 10^{-6} \text{ mol/L}, 1 \sim 10 \text{ } C_{\text{SY}}=(0, 0.4, 1.0, 1.5, 2.0, 2.5, 3.0, 3.5, 4.0, 4.5) \times 10^{-5} \text{ mol/L}$$

In order to study the quenching mechanism, the quenching data was processed according to the Stern-Volmer Eq. (2) [13], and the results were shown in Table 1.

$$I_0 / I = 1 + k_q \tau_0 [L] = 1 + K_{sv} [L] = 1 + K_D [L]$$

(2)

Where, I_0 and I are the fluorescence intensities of TRP in the absence and presence of the SY, respectively. k_q is the bimolecular quenching constant and $[L]$ is the concentration of the quencher, τ_0 is the average lifetime of fluorescence (about 10^{-8} s) and K_{sv} is the Stern-Volmer quenching constant. If the resulting plots exhibit a good linear relationship, this is almost indicative of the static quenching process or dynamic quenching process. Stern-Volmer plots of the fluorescence of TRP quenched by SY at different temperatures are shown in Fig. 3. The good linear relationship reflected the existence of a single annihilation. From Table 1, it could be seen that the k_q value was greater than 2.0×10^{10} L/(mol·s) at different temperatures. The K_{sv} value was inversely correlated with temperatures. The result indicated that the combination process of SY-TRP system was a static quenching process [14].

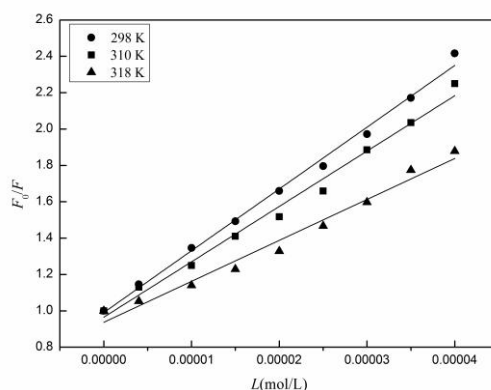


Fig 3 Stern-Volmer plots for the quenching of TRP by SY at different temperatures

$C_{TRP}=4.0 \times 10^{-6}$ mol/L, $1 \sim 10$ $C_{SY}=(0, 0.4, 1.0, 1.5, 2.0, 2.5, 3.0, 3.5, 4.0) \times 10^{-5}$ mol/L

Table 1 Quenching reactive parameters of SY-TRP system at different temperatures

λ_{ex} (nm)	T/(K)	K_{sv} (L/mol·s)	K_q (L/mol)	r_1	K_a (L/mol)	n	r_2
$\lambda_{ex}=280$	298	4.22×10^4	4.22×10^{12}	0.9952	4.26×10^4	1.08	0.9937
	310	3.83×10^4	3.83×10^{12}	0.9923	3.39×10^4	1.06	0.9905
	318	3.06×10^4	3.06×10^{12}	0.9944	2.75×10^4	1.22	0.9964
$\lambda_{ex}=295$	298	3.48×10^4	3.48×10^{12}	0.9922	3.16×10^4	1.17	0.9937
	310	3.02×10^4	3.02×10^{12}	0.9912	2.43×10^4	1.12	0.9928
	318	2.60×10^4	2.60×10^{12}	0.9943	1.82×10^4	0.91	0.9916

r_1 is the linear relative coefficient of $I_0/I \sim [L]$, r_2 is the linear relative coefficient of $\lg [(I_0-I)/I] \sim \lg \{ [L] - n[B_i](I_0-I)/I_0 \}$.

The relationship between fluorescence intensity and the concentration of quencher can usually be described using Eq. (3) [15] to obtain the binding constant (K_a) and the number of binding sites (n):

$$\lg \left(\frac{I_0 - I}{I} \right) = n \lg K_a + n \lg \left\{ [L] - n \frac{I_0 - I}{I_0} [B_i] \right\}$$

(3)

Where $[L]$ and $[B_i]$ are the concentrations of SY and TRP, respectively. On the assumption that n in the bracket is equal to 1, the curve of $\lg(I_0-I)/F$ versus $\lg \{ [L] - n[B_i](I_0-I)/I \}$ is drawn and linearly fitted, then the

value of n can be obtained from the slope of the plot. On the basis of value of n obtained, the binding constant K_a can also be determined. The results were listed in the Table 1. The results showed that all the values of n were approximately equal to 1 at different temperatures, indicating that SY had only one high-affinity binding site when bound to TRP [16], that was, SY and TRP formed a 1:1 complex. When the temperature rose, the binding constant K_a value was in the order of 10^4 and showed a decreasing trend, and the binding ability of SY to TRP was reduced, which further proved that the SY-TRP system was static quenching. Fig.4 showed the involvement of Tyr and Trp residues in TRP. As can be

seen in Fig. 4, the fluorescence quenching curve at $\lambda_{ex}=280$ and 295 nm was separated, and the fluorescence quenching curve of $\lambda_{ex}=280$ nm is lower than that at λ_{ex}

$=295$ nm, implying that both Trp and Tyr residues of TRP participated the reaction and the Trp residue involvement was larger than that of Tyr residue.

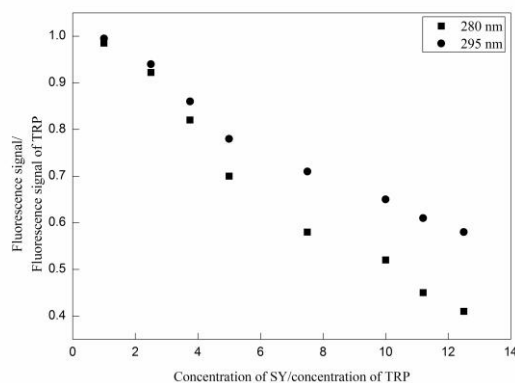


Fig.4 Relative fluorescence curves of the interaction between SY and TRP ($T = 298$ K)

$$C_{TRP}=4.0 \times 10^{-6} \text{ mol/L}, C_{SY} = 4.0 \times 10^{-6} \sim 4.5 \times 10^{-5} \text{ mol/L}$$

3.2 Type of interaction force of SY-TRP system

Generally, the interaction force between the small drug molecule and biological macromolecule includes hydrogen bond, Vander Waals force, electrostatic interactions and hydrophobic force, etc. The type of interaction force in SY-TRP system can be obtained by

the thermodynamic parameters, and calculated by van't Hoff equations [17]. The calculated results were shown in Table 2.

$$R \ln K = \Delta S - \Delta H / T \quad (4)$$

$$\Delta G = \Delta H - T \Delta S \quad (5)$$

Table 2 The thermodynamic parameters of SY-TRP at different temperatures

System	T /(K)	K_a /(L/mol)	ΔH /(kJ/mol)	ΔS /(J/mol·K)	ΔG /(kJ/mol)
$\lambda_{ex}=280$ nm	298	4.26×10^4	-16.91	31.89	-26.41
	310	3.39×10^4		32.18	-26.88
	318	2.75×10^4		31.83	-27.03

Where ΔH and ΔS represent the standard variation of the enthalpy and, respectively, entropy of the binding process. R is the gas constant ($R=8.314$ J/mol·K), T is the absolute temperature. Based on the linear fit plot of $R \ln K_a$ versus $1/T$, the ΔH and ΔS values can be obtained. The results obtained are listed in Table 2. It can be seen from Table 2 that $\Delta G < 0$, indicating that the quenching reaction of SY to TRP was spontaneous; $\Delta S > 0$, suggesting that there was hydrophobic interaction between SY and TRP; $\Delta H < 0$ cannot be used as a sign of inter molecular electrostatic attraction, Ross pointed out that when $\Delta H \approx 0$, $\Delta S > 0$, it could be considered as electrostatic attraction, and $\Delta H < 0$ is considered as the result of hydrogen bonding [18-20]. Therefore, the force between SY and TRP was mainly hydrophobic interaction and hydrogen bonding.

In general, electrostatic force plays a supporting role in the binding of proteins and ligands. However, if electrostatic interactions plays a dominant role in the

binding of proteins to small molecules, the interaction intensity decreases as the salt concentration increases in the system[21]. In order to further verify the existence of

Open Access

electrostatic interaction between SY and TRP, the effect of ionic strength on SY-TRP interaction was discussed.

The concentrations of SY and TRP were fixed, and different concentrations of NaCl were added, and I/I_0 was plotted against C_{NaCl} . The results were shown in Fig. 5. The experimental results showed that the ratio of I/I_0 did

not change significantly when the concentration of NaCl increases, indicating that the combination of SY and TRP was not affected by ionic strength, that is, the SY-TRP system had no obvious electrostatic effect. This conclusion was the same as the conclusion of the thermodynamic constant.

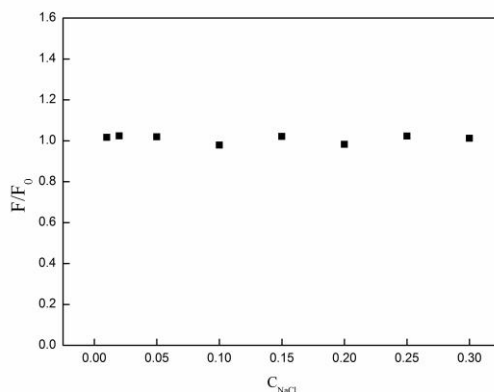


Fig. 5 Fluorescence intensity of SY-TRP system as a function of NaCl concentration ($T=298\text{ K}$)
 $C_{\text{TRP}}=4.0\times 10^{-6}\text{ mol/L}$, $C_{\text{SY}}=1.0\times 10^{-5}\text{ mol/L}$, $C_{\text{NaCl}}=(0, 0.1, 0.2, 0.5, 1.0, 1.5, 2.0, 2.5, 3.0)\times 10^{-1}\text{ mol/L}$

3.3 Conformation study of SY-TRP system

3.3.1 Synchronous fluorescence studies of SY-TRP system

For synchronous fluorescence spectra of proteins, when the $\Delta\lambda$ value between the excitation and emission wavelengths is stabilized at 15 or 60 nm, the synchronous fluorescence gives characteristic information for Tyr or Trp residues[22]. Fig.6 (A and B) showed the effects of SY on the synchronous fluorescence spectra of TRP. It can be seen from Fig. 5 that when $\Delta\lambda=15\text{ nm}$ or $\Delta\lambda=60\text{ nm}$,

the fluorescence intensity of TRP decreased with the increase of SY concentration, showing that Tyr and Trp residues both participated in the interaction of SY with TRP. In addition, the maximum emission wavelength of Tyr and Trp residues had a slightly red shift, suggesting that the microenvironment of these residues became more hydrophobic and polarity enhancement. The results indicated that the SY caused a change in the conformation of the TRP.

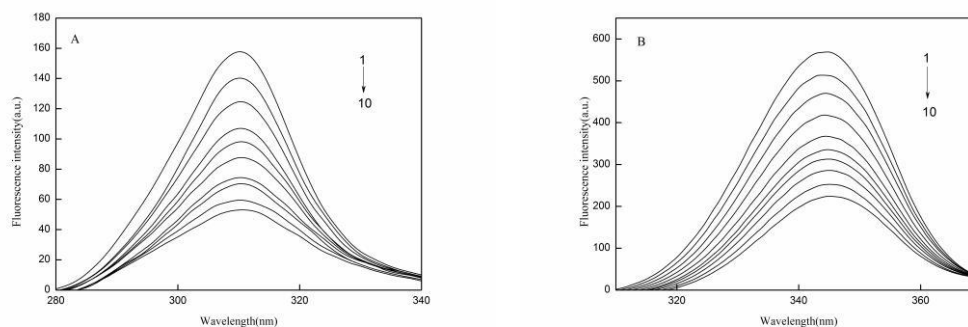


Fig. 6 Synchronous fluorescence spectra of SY-TRP system ($T=298\text{ K}$). (A) $\Delta\lambda=15\text{ nm}$; (B) $\Delta\lambda=60\text{ nm}$
 $C_{\text{TRP}}=4.0\times 10^{-6}\text{ mol/L}$, $1\sim 10\ C_{\text{SY}}=(0, 0.4, 1.0, 1.5, 2.0, 2.5, 3.0, 3.5, 4.0, 4.5)\times 10^{-5}\text{ mol/L}$

3.3.2 UV-vis absorption spectra studies of SY-TRP system

UV-vis absorption spectroscopy can be used to explore structural changes in proteins and to study the formation of protein-ligand complexes. The UV-vis absorption spectra of SY-TRP system was shown in Fig. 7. TRP had two absorption peaks, the strong absorption peak at about 210 nm reflects the framework conformation of the protein, and the weak absorption peak at about 280 nm due to the aromatic amino acids (Trp, Tyr, and Phe)[23]. With gradual addition of SY to TRP solution, the intensity peak of TRP at 210 nm decreased with a red

shift and the intensity of the peak at 280 nm had minimal changes, indicating that the interaction between SY and TRP affected the polarity of microenvironment of Tyr and Trp residues. It made stretch of the peptide chain increase and altered the conformation of the protein [24]. The quenching effect of the excited state protein molecule and the ligand did not change the UV spectrum of the protein, but the UV spectrum of the system has changed, suggesting that the reaction of SY and TRP generated a new complex[25]. This conclusion was consistent with the conclusion of the fluorescence experiment.

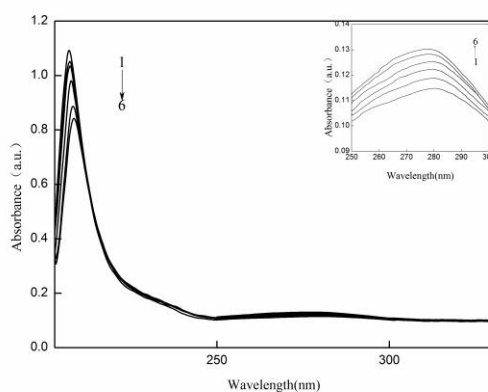


Fig. 7 Absorption spectrum of SY-TRP system ($T=298\text{ K}$)

$$C_{\text{TRP}}=4.0 \times 10^{-6} \text{ mol/L, } 1\sim 6: C_{\text{SY}}=(0, 0.4, 1.0, 1.5, 2.0, 2.5) \times 10^{-5} \text{ mol/L}$$

3.3.3 Circular dichroism spectra studies of SY-TRP system

Circular dichroism spectroscopy (CD) is commonly used to detect changes in the secondary structure of proteins. The CD spectrum of the SY-TRP system is shown in Fig. 8. It can be seen from Fig. 8 that the characteristic peak at 208 nm is the characteristic peak of the α -helix structure in TRP [26]. When the concentration ratio of TRP to SY was 1:0, 1:5 and 1:10, the α -helix content of TRP decreased from 12.10% to 8.71%. As the concentration of SY increased, the absorption intensity of the negative peak gradually decreased, implying that SY caused a change in the secondary structure of TRP, made the protein structure loose. But the peak shape and peak position had not been changed, indicating that the α -helix in the TRP molecule still dominated.

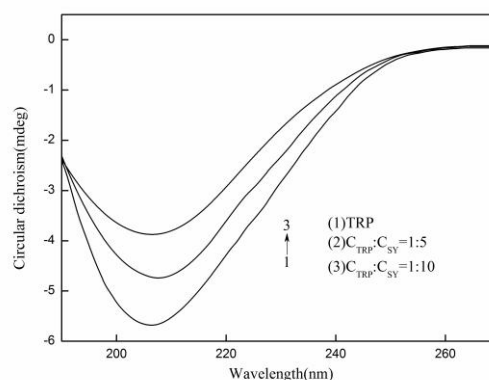


Fig. 8 The circular dichroism spectra of SY-TRP system ($T=298\text{ K}$)

$$C_{\text{TRP}} = 4.0 \times 10^{-6} \text{ mol/L; } C_{\text{SY}} = (2.0, 4.0) \times 10^{-5} \text{ mol/L}$$

3.4 Binding distance of SY-TRP system

Fluorescence resonance energy transfer is an important technology, which has a wide range of applications in the

Open Access

analysis of the interaction between biological macromolecules and small molecules, cell physiology and immune analysis. According to Förster's non-radiative energy transfer theory[27], energy efficiency E , critical energy-transfer distance R_0 ($E=50\%$), the energy donor and the energy acceptor distance r and the overlap integral between the fluorescence emission spectrum of the donor and the absorption spectrum of the acceptor J can be calculated by the following formulas:

$$E = 1 - I/I_0 = R_0^6 / (R_0^6 + r^6) \quad (6)$$

$$R_0^6 = 8.79 \times 10^{-25} K^2 \Phi N^{-4} J \quad (7)$$

$$J = \sum I(\lambda) \varepsilon(\lambda) \lambda^4 \Delta\lambda / I(\lambda) \Delta\lambda \quad (8)$$

Where, K^2 was the orientation factor, Φ was the fluorescence quantum yield of the donor, N was a

refractive index of the medium, $I(\lambda)$ was the fluorescence intensity of the fluorescedonor at wavelength λ and $\varepsilon(\lambda)$ is the molar absorption coefficient of the acceptor at this wavelength. The overlap of UV-vis absorption spectra of SY and the fluorescence emission spectra of TRP ($\lambda_{ex}=280$ nm) were shown in Fig. 9. Under these experimental conditions, it has been reported that $K^2=2/3$, $N=1.336$ and $\Phi=0.118$ [28]. Thus J , E , R_0 and r were calculated and shown in Table 3. The donor-to-acceptor distance $r < 7$ nm, which indicated that there was a non-radiative energy transition in the system [29]. The energy efficiency E decreased and the distance r increased with increasing temperature (Table 3), which resulted in the reduced stability of the binary system and the values of K_a , which was coincident with the result of fluorescence experiment, namely the decreasing trend of K_a with the increasing temperature.

Table 3 Binding parameters between SY-TRP system at different temperatures

$T/(K)$	$E/(%)$	$J/(\text{cm}^3 \cdot \text{L}/\text{mol})$	$R_0/(\text{nm})$	$r/(\text{nm})$
298	12.69	5.16×10^{-16}	1.59	2.20
310	11.47	5.47×10^{-16}	1.62	2.27
318	11.06	5.66×10^{-16}	1.64	2.31

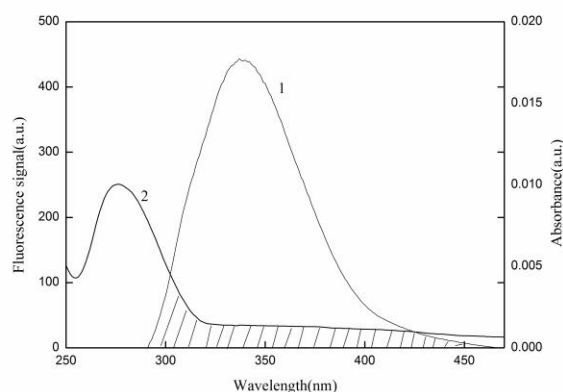


Fig. 9 Fluorescence emission spectra of TRP ($\lambda_{ex} = 280$ nm) (1) and UV absorption spectra of SY (2) ($T=298K$),

$$C_{TRP} = C_{SY} = 4.0 \times 10^{-6} \text{ mol/L}$$

3.5 Molecular docking

Molecular docking method can simulate the interaction between small molecules and proteins at the atomic level, so that it can find small molecules at the target protein binding site and clarify interesting biochemical processes. The best combination mode predicted by the docking software Autodock 4.2.6 was shown in Fig. 10.

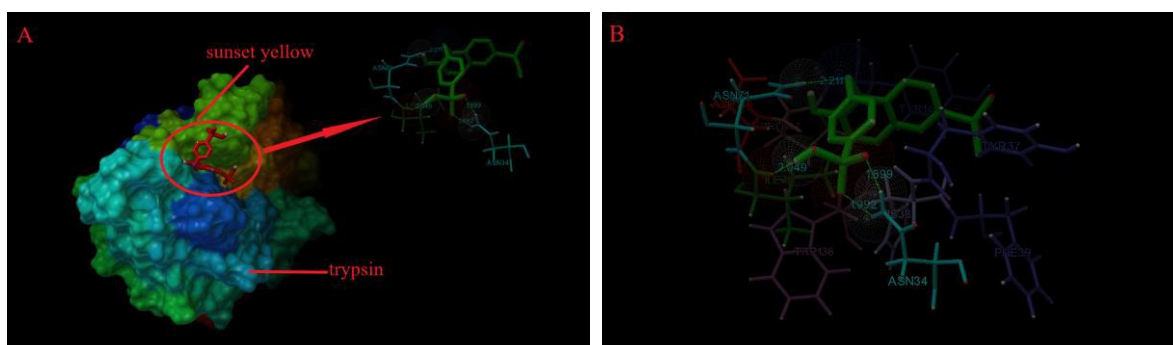


Fig. 10 Computation docking model of the interaction between SY and TRP

(A) SY located within the hydrophobic pocket in TRP (B) Detailed illustration of the amino acid residues lining the binding site in the SY and TRP cavity

Fig. 10(A) showed the optimal combination of SY and TRP. SY and Gly219, Asn143, Ser195, and Gly193 residues formed four hydrogen bonds, and the bond lengths were 1.930 Å, 2.143 Å, 1.791 Å and 1.743 Å, respectively, showing that hydrogen bond played a very important role in the combination of SY and TRP. At the same time, the low free energy binding site of SY on TRP was also given. SY was bound in the hydrophobic cavity of TRP and surrounded by active amino acid residues His57, Ser195 and Asp102, which changed the microenvironment of amino acid residues in the catalytic active center of TRP. Fig. 10(B) showed that SY was surrounded by various kinds of hydrophobic residues such as Pro147, Tyr151, Trp215, Val213, indicating that hydrophobic forces promoted the binding process of SY to TRP. The binding energy obtained from molecular docking for SY and TRP interaction was -26.36 kJ/mol. Whereas, the free energy change calculated from fluorescence quenching results was -26.41 kJ/mol. This difference may be due to exclusion of the solvent in docking simulations or rigidity

of the receptor other than Trp and Tyr residues[30]. The energy data obtained by docking the molecules are listed in Table 4. From Table 4, it could be also seen that the electrostatic energy was very much lower than the sum of Vander Waals energy, hydrogen bonding energy and desolvation free energy in the binding process of SY with TRP, indicating that the main interaction mode between SY and TRP was not electrostatic binding mode. This is also consistent with the effect of ionic strength on the fluorescence experiment of SY-TRP binding. The binding position of SY was near to that of Tyr151 and Trp215, suggesting that both Tyr and Trp residues participated in the reaction, which was consistent with the fluorescence quenching experiment. Through fluorescence experiments and molecular docking, it could be inferred that SY and TRP were combined by hydrophobic force and hydrogen bonding, resulting in static quenching of TRP fluorescence. Therefore, the docking technique showed the same result, confirmed each other and got the final conclusion.

Table 4 Docking energy of SY-TRP system (unit: kJ/mol)

Protein PDB ID	ΔG_0	ΔE_1	ΔE_2	ΔE_3
2ZQ1	-26.36	-35.10	-33.93	-1.17

ΔG_0 is the binding energy in the binding process.

ΔE_1 denotes intermolecular interaction energy, which is a sum of van der Waals energy, hydrogen bonding energy, desolvation free energy and electrostatic energy.

ΔE_2 is the sum of van der Waals energy, hydrogen bonding energy and desolvation free energy.

ΔE_3 is the electrostatic energy.

IV. CONCLUSION

In this paper, the interaction mechanism between SY and TRP was studied by using multiple spectroscopy methods and molecular docking simulation techniques under simulated physiological conditions. During the fluorescence spectroscopic and computational analysis, SY quenched the fluorescence of TRP effectively to form a complex with only one site of protein mainly through hydrophobic force and hydrogen bond. The microenvironment and conformation of TRP were also changed by the bound SY as indicated by the UV-Visible absorption, synchronous fluorescence and CD spectra. Experiments have proved that SY has a strong binding ability to TRP, which provides theoretical guidance for further understanding the toxicity of colorants to human and further studies are needed to provide for health risk assessment of food colorants.

ACKNOWLEDGMENTS

The authors gratefully acknowledge the financial support of National Natural Science Foundation of China (No. 21375032).

REFERENCES

- [1] Liu, Y.Y.; Zhang, G.W.; Liao, Y.G.; Wang, Y.P. Binding characteristics of psoralen with trypsin: Insights from spectroscopic and molecular modeling studies. *Spectrochim. Acta. A. Mol. Biomol. Spectrosc.* 2015, *151*, 498-505. doi: 10.1016/j.saa.2015.07.018.
- [2] He, W.; Dou, H.J.; Zhang, L.; Wang, L.J.; Wang, R.Y.; Chang, J.B. Spectroscopic study on the interaction of Trypsin with Bicyclol and analogs. *Acta. A. Mol. Biomol. Spectrosc.* 2014, *118*, 510-519. doi: 10.1016/j.saa.2013.09.027.
- [3] Ding, K.K.; Zhang, H.X.; Wang, H.F.; Lv, X.; Pan, L.M.; Zhang, W.J.; Zhuang, S.L. Atomic-scale investigation of the interactions between tetrabromobisphenol A, tetrabromobisphenol S and bovine trypsin by spectroscopies and molecular dynamics simulations. *J. Hazard. Mater.* 2015, *299*, 486-494. doi:10.1016/j.jhazmat.2015.07.050.
- [4] Almeida, M.R.; Stephani, R.; Santos, H.F.; Oliveira, L.F. Spectroscopic and theoretical study of the "azo"-dye E124 in condensate phase: evidence of a dominant hydrazo form. *J. Phys. Chem. A.* 2009, *114*, 526-534. doi: 10.1021/jp907473d
- [5] Perez-Urquiza, M.; Beltran, J. Determination of dyes in foodstuffs by capillary zone electrophoresis. *J. Chromatogr. A.* 2000, *898*, 271-275. doi: 10.1016/S0021-9673(00)00841-4.
- [6] McCann, D.; Barrett, A.; Cooper, A.; Crumpler, D.; Dalen, L.; Grimshaw, K.; Kitchin, E.; Lok, K.; Porteous, L.; Prince, E.; Sonuga-Brake, E.; Warner, J.O.; Stevenson, J. Food additives and hyperactive behaviour in 3-year-old and 8/9-year-old children in the community: a randomised, double-blinded, placebo-controlled trial. *Lancet.* 2007, *370*, 1560-1567. doi: 10.1016/s0140-6736(07)61306-3
- [7] Dorraji, P.S.; Jalali, F. Electrochemical fabrication of a novel ZnO/cysteic acid nanocomposite modified electrode and its application to simultaneous determination of sunset yellow and tartrazine. *Food. Chem.* 2017, *227*, 73-77. doi: 10.1016/j.foodchem.2017.01.071
- [8] Mohseni-Shahri, F.S.; Moeinpour, F.; Nosrati, M. Spectroscopy and molecular dynamics simulation study on the interaction of sunset yellow food additive with trypsin. *Int. J. Biol. Macromol.* 2018, *115*, 273-280. doi: 10.1016/j.ijbiomac.2018.04.080.
- [9] Liu, Z.D.; Han, D.Q.; Yang, W.W.; Shao, S. S.; Sun, Q.S. Interactions of Bovine Serum Albumin with Lemon Yellow and Sunset Yellow Studied by Fluorescence Spectroscopy. *J. Food. Sci.* 2014, *35*, 128-131.
- [10] Ma, L.H.; Liu, B.S.; Wang, C.D.; Zhang, H.C.; Cheng, X. The interaction mechanism of nifedipine and pepsin. *Mon. Chem.* 2018, *149*, 2123-2130. doi : 10.1007/s00706-018-2269-9.
- [11] Elmas, G.; Esra, Y. Fluorescence interaction and determination of sulfathiazole with trypsin. *J. Fluoresc.* 2014, *24*, 1439-1445. doi: 10.1007/s10895-014-1427-7.
- [12] Safarnejad, A.; Shaghghi, M.; Dehghan, G.; Soltani, S. Binding of carvedilol to serum albumins investigated by

- multi-spectroscopic and molecular modeling methods. *J. Lumin.* 2016, *176*, 149-158. doi : 10.1016/j.jlumin.2016.02.001.
- [13] Tian, Z.Y.; Zang, F.L.; Luo, W.; Zhao, Z.H.; Wang, Y.Q.; Xu, X.J. Spectroscopic study on the interaction between mononaphthalimide spermidine (MINS) and bovine serum albumin (BSA). *J. Photochem. Photobiol. B-Biol.* 2015, *142*, 103-109. doi: 10.1016/j.jphotobiol.2014.10.013.
- [14] Cao, S.N.; Liu, B.S.; Li, Z.Y.; Zong, B.H. A fluorescence spectroscopic study of the interaction between Glipizide and bovine serum albumin and its analytical application. *J. Lumin.* 2014, *145*, 94-99. doi : 10.1016/j.jlumin.2013.07.026.
- [15] Cheng, F.Q.; Wang, Y.P.; Li, Z.P.; Dong, C. Fluorescence study on the interaction of human serum albumin with bromsulphalein. *Spectrochim. Acta. A. Mol. Biomol. Spectrosc.* 2006, *65*, 1144-1147. doi : 10.1016/j.saa.2006.01.024.
- [16] Basken, N. E.; Green, M.A. Cu(II) bis(thiosemicarbazone) radiopharmaceutical binding to serum albumin: further definition of species dependence and associated substituent effects. *Nucl. Med. Biol.* 2009, *36*, 495-504. doi: 10.1016/j.nucmedbio.2009.02.006.
- [17] Guo, J.; Zhong, R.; Li, W.R.; Liu, Y.S. Interaction study on bovine serum albumin physically binding to silver nanoparticles: Evolution from discrete conjugates to protein coronas. *Appl. Surf. Sci.* 2015, *359*, 82-88. doi: 10.1016/j.apsusc.2015.09.247.
- [18] Rehman, S.U.; Sarwar, T.; Ishqi, H.M.; Husain, M.A.; Hasan, Z.; Tabish, M. Deciphering the interactions between chlorambucil and calf thymus DNA: A multi-spectroscopic and molecular docking study. *Arch. Biochem. Biophys.* 2015, *566*, 7-14. doi : 10.1016/j.abb.2014.12.013.
- [19] Ross, P.D.; Subramanian, S. Thermodynamics of protein association reactions: forces contributing to stability. *Biochemistry.* 1981, *20*, 3096-3102. doi : 10.1021/bi00514a017.
- [20] Zhou, H.; Bi, S.; Wang, Y.; Zhao, T. Characterization of the binding of paylean and DNA by fluorescence, UV spectroscopy and molecular docking techniques. *Lumin.* 2016, *31*, 1013-1019. doi: 10.1002/bio.3066.
- [21] Azimi, O.; Emami, Z.; Salari, H.; Chamani, J. Probing the interaction of human serum albumin with norfloxacin in the presence of high-frequency electromagnetic fields: fluorescence spectroscopy and circular dichroism investigations. *Molecules.* 2011, *16*, 9792-9818. doi : 10.3390/molecules16129792.
- [22] Hu, X.X.; Yu, Z.Y.; Liu, R.T. Spectroscopic investigations on the interactions between isopropanol and trypsin at molecular level. *Spectrochim. Acta. A. Mol. Biomol. Spectrosc.* 2013, *108*, 50-54. doi : 10.1016/j.saa.2013.01.072.
- [23] Liu, Y.; Chen, M. M.; Song, L. Comparing the effects of Fe(III) and Cu(II) on the binding affinity of erlotinib to bovine serum albumin using spectroscopic methods. *J. Lumin.* 2013, *134*, 515-523. doi : 10.1016/j.jlumin.2012.07.036.
- [24] Cagnardi, P.; Villa, R.; Gallo, M.; Locatelli, C.; Carli, S.; Moroni, P.; Zonca, A. Cefoperazone sodium preparation behavior after intramammary administration in healthy and infected cows. *J. Dairy Sci.* 2010, *93*, 4105-4110. doi: 10.3168/jds.2010-3379.
- [25] Liu, Y.Y.; Zhang, G.W.; Liao, Y.G.; Wang, Y.P. Binding characteristics of psoralen with trypsin: Insights from spectroscopic and molecular modeling studies. *Spectrochim. Acta. A. Mol. Biomol. Spectrosc.* 2015, *151*, 498-505. doi: 10.1016/j.saa.2015.07.018.
- [26] Gabb, H.A.; Jackson, R.M.; Sternberg, M.J. Modelling protein docking using shape complementarity, electrostatics and biochemical information. *J. Mol. Biol.* 1997, *272*, 106-120. doi: 10.1006/jmbi.1997.1203.
- [27] Jin, J.; Zhang, X. Spectrophotometric studies on the interaction between pazufloxacin mesilate and human serum albumin or lysozyme. *J. Lumin.* 2008, *128*, 81-86. doi: 10.1016/j.jlumin.2007.05.008.
- [28] Bertucci, C.; Domenici, E. Reversible and Covalent Binding of Drugs to Human Serum Albumin: Methodological Approaches and Physiological Relevance. *Curr. Med. Chem.* 2002, *9*, 1463-1481. doi: 10.2174/0929867023369673.
- [29] Manivel, A.; Anandan, S. Spectral interaction between silica coated silver nanoparticles and serum albumins. *Colloid. Surface. A.* 2012, *395*, 38-45. doi :

Open Access

10.1016/j.colsurfa.2011.12.001.

- [30] Jana, S.; Dalapati, S.; Ghosh, S.; Guchhait, N. Study of microheterogeneous environment of protein Human Serum Albumin by an extrinsic fluorescent reporter: a spectroscopic study in combination with Molecular Docking and Molecular Dynamics Simulation. *J. Photochem. Photobiol. B-Biol.* 2012, *112*, 48-58. doi: 10.1016/j.jphotobiol.2012.04.007.